Contribution from the Departments of Chemistry, University of Florence, Florence, Italy, and University of California, Irvine, California

EPR Spectra of Bis(nitroxyl) Adducts of Bis(hexafluoroacetylacetonato)manganese(II)

C. Benelli,[1a] D. Gatteschi,*[1a] C. Zanchini,[1a] R. J. Doedens,[1b] M. H. Dickman,[1b] and L. C. Porter[1b]

Received February 18, 1986

The EPR spectra of the bis(nitroxyl) adducts $Mn(F_6acac)_2(tempo)_2$ (I) and $Mn(F_6acac)_2(proxyl)_2$ (II) (F_6acac = hexafluoroacetylacetonato; tempo = 2,2,6,6-tetramethylpiperidinyl-1-oxy; proxyl = 2,2,5,5-tetramethylpyrrolidinyl-1-oxy) were recorded in the range of temperature 4.2–300 K. The spectra are temperature-dependent, in agreement with previous magnetic susceptibility data, which indicated the thermal population of one $S = {}^3/_2$, two $S = {}^5/_2$, and one $S = {}^7/_2$ total spin states. At low temperature, single-crystal spectra were obtained at both X- and Q-band frequencies, which allowed us to obtain the **D** tensors for the quartet states of both I and II. Polycrystalline powder spectra of the two compounds at room temperature provided an estimate of D and E/D for the first excited sextuplet. These data are used to discuss the isotropic exchange and the anisotropic spin–spin interaction in I and II.

Introduction

Complexes in which a transition-metal ion is coordinated to a nitroxyl radical are excellent tests of the nature of the interaction between the free spins on the organic radical and those on a paramagnetic metal center.[2-5] In principle the unpaired electrons on the radicals can be strongly coupled with those of the metal ions, yielding diamagnetic behavior at all accessible temperatures.[6,7] At the other limit the orbitals containing the unpaired spins can be orthogonal to each other in such a way that the highest spin multiplicity state will have lowest energy, or, in other words, a ferromagnetic coupling between the two centers can be developed.[5,8,9] Between these two limits it is possible to have intermediate situations in which several different spin states are thermally populated. The possibility of such a large variation in the coupling is mainly due to the weakness of the interaction between the transition-metal ion and the radical, as a consequence of which states other than the spin-paired one may be stable. These systems are therefore very flexible ones and in principle can give rise to novel magnetic behavior.

The Irvine group recently reported the preparation, structures, and magnetic properties of two bis(nitroxyl) adducts of bis(hexafluoroacetylacetonato)manganese(II), $Mn(F_6acac)_2(tempo)_2$ (I) and $Mn(F_6acac)_2(proxyl)_2$ (II) (F_6acac = hexafluoroacetylacetonato; tempo = 2,2,6,6-tetramethylpiperidinyl-1-oxy; proxyl = 2,2,5,5-tetramethylpyrrolidinyl-1-oxy).[9] In both I and II the manganese(II) ion is octahedrally coordinated by two F_6acac ligands, which occupy equatorial positions, and by two nitroxyl ligands, which occupy axial positions. The temperature dependence of the magnetic susceptibility was well represented by a model in which the coupling between the manganese(II) ion, $S_{Mn} = {}^5/_2$, and the two radicals, $S_r = {}^1/_2$, yields a ground $S = {}^3/_2$ level, with two $S = {}^5/_2$ and one $S = {}^7/_2$ excited states which are thermally populated. The coupling constant, defined by the Hamiltonian $\mathbf{H} = J\mathbf{S}_r\cdot\mathbf{S}_{Mn}$, was found to be 158 cm^{-1} for I and 210 cm^{-1} for II.

In order to gain a deeper insight into the electronic structure of these compounds, we decided to record the EPR spectra of I and II over a large temperature range with the aim of characterizing as many spin states as possible.

Experimental Section

The complexes were obtained by the procedure previously described.[10] EPR-suitable single crystals of I and II were oriented with a Philips PW 1100 diffractometer and were found to correspond to the described structure with well-developed (100) and ($\bar{1}00$) faces. EPR variable-temperature spectra at X- and Q-band frequencies were recorded with Bruker ER200 and Varian E9 spectrometers equipped with standard apparatus down to liquid-nitrogen temperature and with an Oxford Instruments ESR9 continuous-flow cryostat below that limit.

Single-crystal spectra were obtained by mounting the crystals on a Perspex rod. At X-band the rod was rotated with a one-circle goniometer, while at Q-band the magnet was rotated.

Results

The polycrystalline powder EPR spectra of I and II recorded at X-band frequency in the range 4.2–300 K are shown in Figures 1 and 2. Both sets of spectra show a marked temperature dependence: at low temperature essentially two features, similar to those expected for an axial $S = {}^1/_2$ spin state, centered at $g_\parallel = 2$ and $g_\perp = 4$, are observed. The high-temperature spectra are much more complicated with features spread out in the range 0–0.8 T. It is remarkable that the low-temperature features are not easily identified in the room-temperature spectra.

The Q-band spectra (Figures 3 and 4) recorded in the range 140–300 K display similar behavior, in the sense that the number of observed features increases with temperature. The spectra at 140 K are however more complicated than those recorded at X-band frequency at low temperature. In addition to features in the $g = 2$ and $g = 4$ regions, there are also some absorptions at very low fields (0–200 mT).

Single-crystal spectra were recorded for I at 4.2 K at X-band frequency and at 140 K at Q-band frequency. The angular dependence of the transition fields in the three orthogonal planes XZ, XY, and YZ are shown in Figures 5 and 6. X, Y, and Z are laboratory axes, with X parallel to a^* and Z orthogonal to the $01\bar{1}$ face. Since the crystals are monoclinic, two independent molecules are expected to resonate in the above planes, but only in the YZ plane are the absorption fields expected to be symmetric around the b and c axes, as experimentally verified. These data show that no major structural change occurs on lowering temperature.

At X-band frequency the resonances are observed in the 140–350-mT range, but in some angular orientations high-field resonances (600–1000 mT) are also observed.

The room-temperature spectra are very complicated, with many overlapping resonances, which make a detailed analysis of the spectra practically impossible. However, in the XY and XZ planes a transition could be followed in the whole angular range. The resonance field was found to vary from 290 to 650 mT. In order to check if the former transition, which presumably is responsible for the strong feature at 290 mT in the powder spectra, corresponds to the one seen in the low-temperature spectrum, the spectra with the external magnetic field parallel to X were recorded in the range 140–300 K. It is apparent from Figure 7 that increasing temperature leads to the appearance of a new transition. Therefore, the signal at 290 mT does not belong to the low-temperature spectrum.

Single-crystal spectra of II were recorded at 140 K, at both X- and Q-band frequencies. The angular dependence of the

(1) (a) University of Florence. (b) University of California.
(2) Benelli, C.; Gatteschi, D.; Zanchini, C. *Inorg. Chem.* **1984**, *23*, 798.
(3) Dickman, M. H.; Doedens, R. J. *Inorg. Chem.* **1983**, *22*, 1591.
(4) Grand, A.; Rey, P.; Subra, R. *Inorg. Chem.* **1983**, *22*, 391.
(5) Anderson, O. P.; Kuechler, T. C. *Inorg. Chem.* **1980**, *19*, 1417.
(6) Dickman, M. H.; Doedens, R. J. *Inorg. Chem.* **1981**, *20*, 2677.
(7) Lim, Y. Y.; Drago, R. S. *Inorg. Chem.* **1972**, *11*, 1334.
(8) Benelli, C.; Gatteschi, D.; Carnegie, D. W., Jr.; Carlin, R. L. *J. Am. Chem. Soc.* **1985**, *107*, 2560.
(9) Bencini, A.; Benelli, C.; Gatteschi, D.; Zanchini, C. *J. Am. Chem. Soc.* **1984**, *106*, 5813.
(10) Dickman, M. H.; Porter, L. C.; Doedens, R. J., submitted for publication.

0020-1669/86/1325-3453$01.50/0

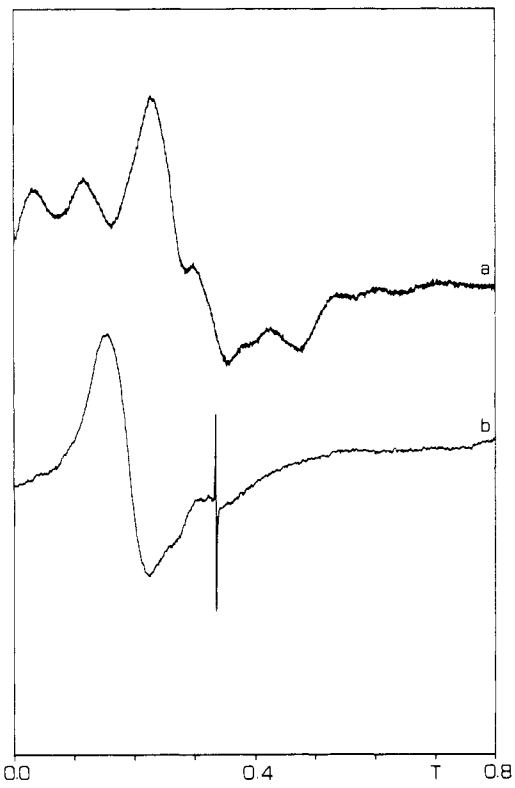

Figure 1. Polycrystalline powder EPR spectra of $Mn(F_6acac)_2(tempo)_2$ (I) recorded at X-band frequency: (a) 300 K; (b) 4.2 K.

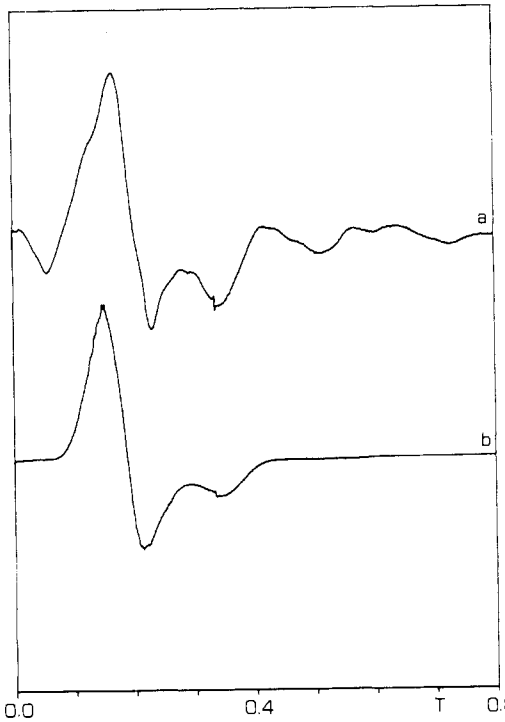

Figure 2. Polycrystalline powder EPR spectra of $Mn(F_6acac)_2(proxyl)_2$ (II) recorded at X-band frequency: (a) 300 K; (b) 4.2 K.

transition fields in the *XY*, *XZ*, and *YZ* planes are shown in Figures 8 and 9. The same general comments as for I apply also in this case.

Discussion

Analysis of the EPR Spectra. The interpretation of the EPR spectra of I and II started from the low-temperature data, since they are much simpler than the others. This is consistent with magnetic susceptibility data which showed that in both complexes the coupling between the manganese(II) ions and the radicals is

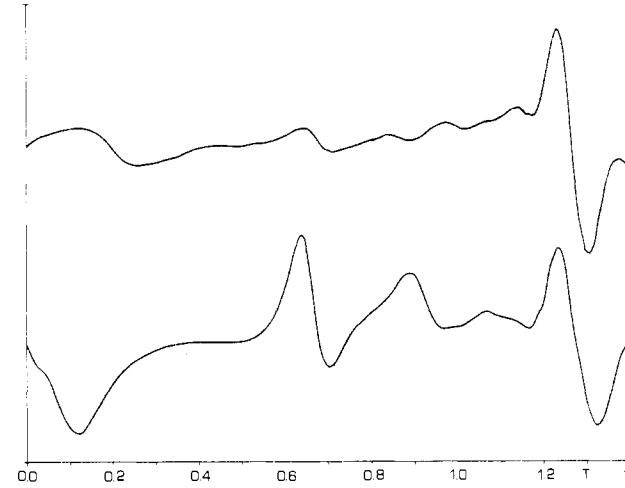

Figure 3. Polycrystalline powder EPR spectra of $Mn(F_6acac)_2(tempo)_2$ (I) recorded at Q-band frequency: (a) 300 K; (b) 140 K.

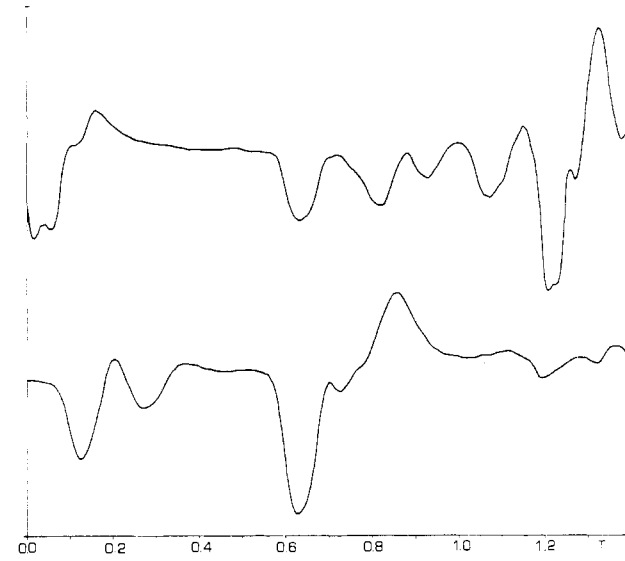

Figure 4. Polycrystalline powder EPR spectra of $Mn(F_6acac)_2(proxyl)_2$ (II) recorded at Q-band frequency: (a) 300 K; (b) 140 K.

antiferromagnetic.[10] The suggested order of levels and the energy separations are shown in Figure 10. The ESR data confirm that the $S = {}^3/_2$ state is the only populated state at temperatures lower than 140 K: indeed, the $g_\parallel \simeq 2$ and $g_\perp \simeq 4$ pattern observed at X-band frequency is in agreement with an axial zero-field splitting that is larger than the microwave quantum, $D > h\nu_X$.[11] Under these conditions the only transitions that can be observed are those within the $M_S = \pm{}^1/_2$ Kramers doublet. The low-temperature Q-band spectra, on the other hand, show more transitions, suggesting that at this frequency the microwave quantum is larger than D. Since transitions are observed at very low fields, D is expected to be close to ${}^1/_2 h\nu_Q$. The X- and Q-band spectra therefore can be interpreted by assuming that $D \simeq 0.6$ cm^{-1}.[12]

The single-crystal X-band spectra of both I and II at low temperature were fit by assuming that the transitions are within the same Kramers doublet, with an effective $S = {}^1/_2$ spin. The calculated best-fit curves are shown in Figures 5 and 8. The principal g values and directions are shown in Table I. The lowest g value (2.00 for I and 2.04 for II) is observed roughly parallel to the Mn–O_1(nitroxide oxygen) direction, while the other two g values approximately bisect the Mn–O bonds.

The observed g values are effective g values, which can be related to the true g values of the $S = {}^3/_2$ state according to the

(11) Bencini, A.; Gatteschi, D. *Transition Met. Chem. (N.Y.)* **1982**, *8*, 1.
(12) Pedersen, E.; Toftlund, H. *Inorg. Chem.* **1974**, *13*, 1603.

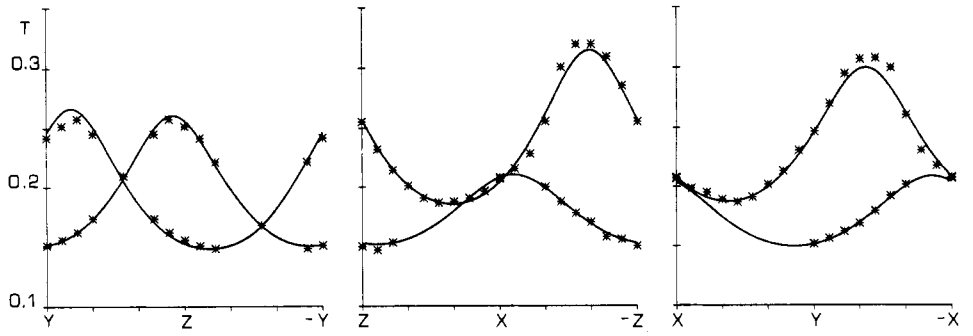

Figure 5. Angular dependence of the transition fields of $Mn(F_6acac)_2(tempo)_2$ (I) at X-band frequency at 4.2 K, in three orthogonal planes. X, Y, and Z are laboratory axes, with X parallel to a^* and Z orthogonal to the $01\bar{1}$ face.

Table I. Principal g Values and Directions for $Mn(F_6acac)_2(tempo)_2$ (I) and $Mn(F_6acac)_2(proxyl)_2$ (II) at X- and Q-Band Frequencies for the Two Magnetically Nonequivalent Sites in the Unit Cell[a]

$Mn(F_6acac)_2(tempo)_2$ (I)

Site A

X-band (T = 4.2 K)			Q-band (T = 140 K)		
g_1 = 3.48 (2)	g_2 = 4.31 (2)	g_3 = 1.93 (3)	g_1 = 2.73 (4)	g_2 = 3.93 (2)	g_3 = 1.23 (5)
−0.823 (8)	0.19 (3)	−0.533 (3)	−0.821 (5)	0.02 (2)	−0.570 (8)
0.13 (4)	0.979 (5)	0.156 (5)	−0.08 (3)	0.985 (3)	0.152 (7)
−0.552 (4)	−0.06 (2)	0.831 (2)	−0.564 (9)	−0.17 (2)	0.807 (6)

Site B

X-band (T = 4.2 K)			Q-band (T = 140 K)		
g_1 = 3.46 (3)	g_2 = 4.32 (3)	g_3 = 1.90 (4)	g_1 = 2.78 (6)	g_2 = 3.97 (4)	g_3 = 1.27 (6)
0.848 (3)	−0.041 (3)	−0.528 (4)	0.805 (6)	−0.08 (2)	−0.586 (8)
0.52 (1)	0.25 (2)	0.815 (3)	0.57 (1)	0.34 (2)	0.742 (7)
0.10 (4)	−0.966 (4)	0.236 (5)	0.14 (2)	−0.935 (5)	0.324 (7)

$Mn(F_6acac)_2(proxyl)_2$ (II)

Site A

X-band (T = 140 K)			Q-band (T = 140 K)		
g_1 = 3.80 (8)	g_2 = 4.43 (8)	g_3 = 1.98 (7)	g_1 = 3.15 (4)	g_2 = 3.98 (2)	g_3 = 1.45 (2)
−0.58 (4)	0.40 (6)	−0.705 (6)	−0.74 (4)	0.18 (3)	−0.65 (5)
0.40 (9)	0.90 (4)	0.18 (1)	0.19 (4)	0.98 (4)	0.05 (4)
−0.70 (2)	0.18 (7)	0.687 (7)	−0.64 (6)	0.08 (2)	0.76 (2)

Site B

X-band (T = 140 K)			Q-band (T = 140 K)		
g_1 = 3.76 (6)	g_2 = 4.49 (4)	g_3 = 2.11 (6)	g_1 = 3.15 (5)	g_2 = 3.97 (4)	g_3 = 1.47 (4)
0.68 (2)	0.26 (5)	−0.687 (6)	0.75 (2)	0.15 (2)	−0.65 (6)
0.725 (9)	−0.08 (6)	0.684 (6)	0.66 (4)	−0.10 (6)	0.74 (5)
−0.12 (7)	0.96 (1)	0.242 (8)	−0.04 (5)	0.98 (7)	0.17 (3)

[a] The directions are given by their direction cosines referred to the orthogonal crystal axes X, Y, and Z with X parallel to a^* and Z orthogonal to the $01\bar{1}$ face.

reported relations.[13] Since both the manganese(II) and the radicals have practically isotropic g's, close to 2, the observed anisotropy of $g_\perp$ must be due to the rhombic component of the zero-field splitting. Using the reported formulas and isotropic g's, we calculated E/D close to 0.1 for both I and II.

The corresponding Q-band spectra were analyzed simply by looking at the transition fields along the X, Y, and Z molecular axes and comparing them with the observed features in the polycrystalline powder spectra. Although this procedure is not rigorous, we felt it could be appropriate in the present case, where we merely want to estimate the zero-field splitting parameter. Satisfactory reproduction of the transition fields at Q-band frequency could be obtained for $D = 0.63 \pm 0.01$ cm^{-1} and $E/D = 0.115 \pm 0.01$ for I, $D = 0.65 \pm 0.01$ cm^{-1} and $E/D = 0.18 \pm 0.02$ for II, and $g = 2$ for both the complexes, in agreement with the predictions made above.

With these D values the transition fields at X-frequency are predicted to be located at $g_\perp \simeq 4$ and $g_\parallel \simeq 2$, with additional features at 0.647 and 0.98 T, as observed in the single-crystal spectra.

The additional features seen in the room-temperature spectra are assigned to the transitions within the lower $S = {}^5/_2$ state. The X-band spectra in particular show some new features at very low fields, suggesting that either $D \simeq {}^1/_2 h\nu_X$ or $D \simeq {}^1/_4 h\nu_X$. The fact that the Q-band spectra show additional features only in the $g = 2$ region suggests that the latter hypothesis is correct.[14,15]

Spin Hamiltonian Parameters. The spin Hamiltonian parameters for the cluster of three spins, $S_r = S_r = {}^1/_2$ and $S_{Mn} = {}^5/_2$, can be easily expressed as a function of the corresponding parameters for the individual spins, with use of well-established vector-coupling techniques.[16] Since the **g** tensors of both the

(13) Pilbrow, J. R. *J. Magn. Reson.* **1978**, *31*, 479

(14) Dowsing, R. D.; Gibson, J. F. *J. Chem. Phys.* **1969**, *50*, 294.
(15) Aasa, R. J. *J. Chem. Phys.* **1970**, *52*, 3919.

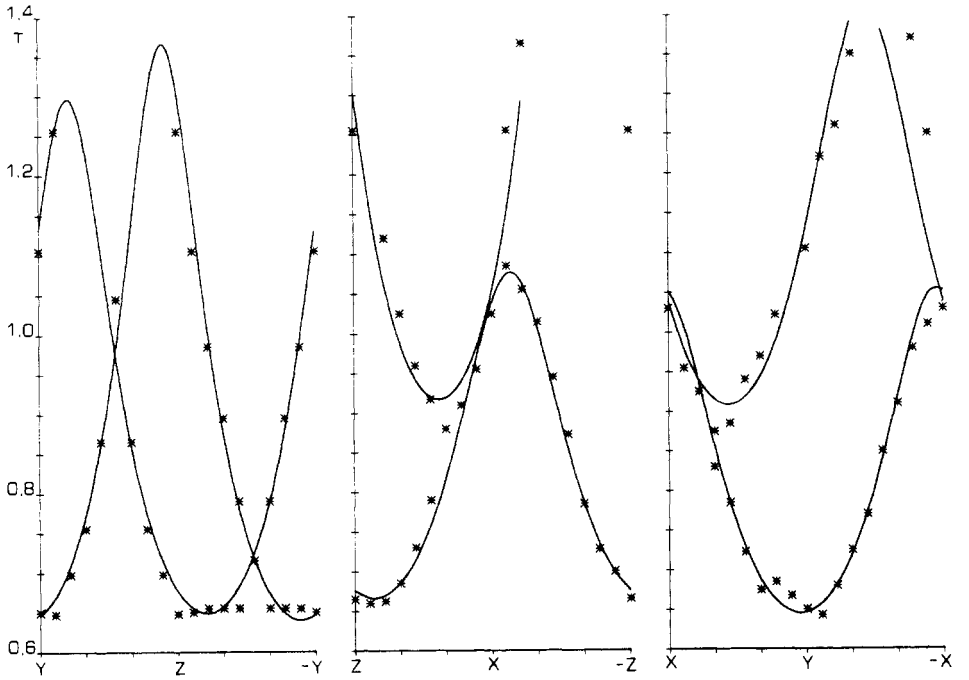

Figure 6. Angular dependence of the transition fields of $Mn(F_6acac)_2(tempo)_2$ (I) at Q-band frequency at 140 K, in three orthogonal planes. X, Y, and Z are laboratory axes, with X parallel to a^* and Z orthogonal to the $01\bar{1}$ face.

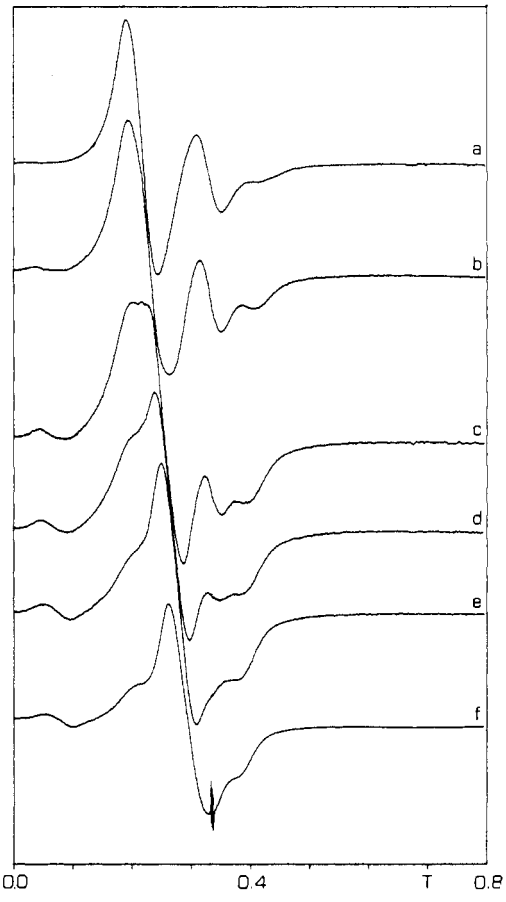

Figure 7. Variable-temperature single-crystal EPR spectra of $Mn(F_6acac)_2(tempo)_2$ (I) recorded with the static magnetic field parallel to X at X-band frequency: (a) 140 K; (b) 175 K; (c) 200 K; (d) 220 K; (e) 260 K; (f) 300 K.

manganese(II) ion and the organic radicals are expected to be quasi-isotropic and to be very close to 2, the **g** tensor of the spin cluster is expected to be quasi-isotropic and close to 2. The zero-field splitting tensors, on the other hand, are expected to be given by the relations

$$\mathbf{D}(^7/_2) = {}^{10}/_{42}D_{Mn-r} + {}^1/_{42}D_{r-r} + {}^{10}/_{21}D_{Mn}$$

$$\mathbf{D}(^5/_2,1) = {}^8/_{35}D_{Mn-r} - {}^2/_{35}D_{r-r} + {}^{23}/_{35}D_{Mn}$$

$$\mathbf{D}(^3/_2) = -{}^{14}/_{30}D_{Mn-r} + {}^1/_{30}D_{r-r} + {}^{28}/_{15}D_{Mn}$$

$$\mathbf{D}(^5/_2,0) = D_{Mn}$$

where D_{Mn} is the zero-field splitting of the individual manganese ion and D_{Mn-r} and D_{r-r} are the exchange- and dipolar-determined contributions originating from the interaction of the radical with the manganese ion and with the other radical, respectively. The labels 1 and 0 for the two $S = {}^5/_2$ states indicate the intermediate spin obtained by first coupling the two radicals.

D_{Mn} cannot be known a priori, but a reasonable estimate, by comparison with literature data on manganese complexes,[11,17,18] suggests a value close to 0.1 cm^{-1} for this parameter. D_{Mn-r} and D_{r-r} are in principle determined by both dipolar and exchange interactions.[19] Since, however, for both the radicals and the manganese ions spin–orbit coupling effects are small, as shown by the g values close to 2, the exchange interaction can be safely neglected.

The magnetic dipolar interaction in the present case cannot be accurately calculated within the point dipolar approximation, because the spin on the radicals is largely delocalized on both in the nitrogen and oxygen atoms, and the manganese–oxygen distance is very short.[20,21] It seems reasonable to assume however that it is dominated by D_{Mn-r}, D_{r-r} being much smaller due to the much larger distance. Also it can be assumed that a first approximation to D_{zz}^{dip} can be obtained by the corresponding value observed for $Cu(F_6acac)_2(tempol)$[9] (tempol = 4-hydroxy-2,2,6,6-tetramethylpiperidinyl-1-oxy).

(16) Gatteschi, D.; Bencini, A. In *Magneto-Structural Correlations in Exchange Coupled Systems*; Gatteschi, D., Kahn, O., Willett, R. W., Eds.; Reidel: Dordrecht, Holland, 1985; p 241.

(17) Birdy, R. B.; Goodgame, M. *Inorg. Chem.* **1979**, *18*, 472.

(18) Dowsing, R. D.; Gibson, J. F.; Goodgame, M.; Hayward, P. J. *J. Chem. Soc. A* **1969**, *187*.

(19) Owen, J.; Harris, E. A. In *Electron Paramagnetic Resonance*; Geschwind, S., Ed.; Plenum: New York, 1972; p 427.

(20) *Spin Labeling: Theory and Applications*; Berliner, L. J., Ed.; Academic: New York, 1976.

(21) Nardenskiald, L.; Laraksonem, A.; Kowalewski, J. *J. Am. Chem. Soc.* **1982**, *104*, 379.

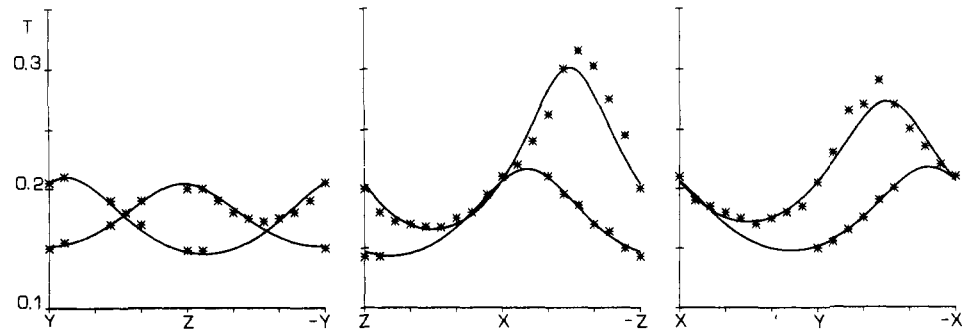

Figure 8. Angular dependence of the transition fields of $Mn(F_6acac)_2(proxyl)_2$ (II) at X-band frequency at 140 K, in three orthogonal planes. *X*, *Y*, and *Z* are laboratory axes, with *X* parallel to a^* and *Z* orthogonal to the $01\bar{1}$ face.

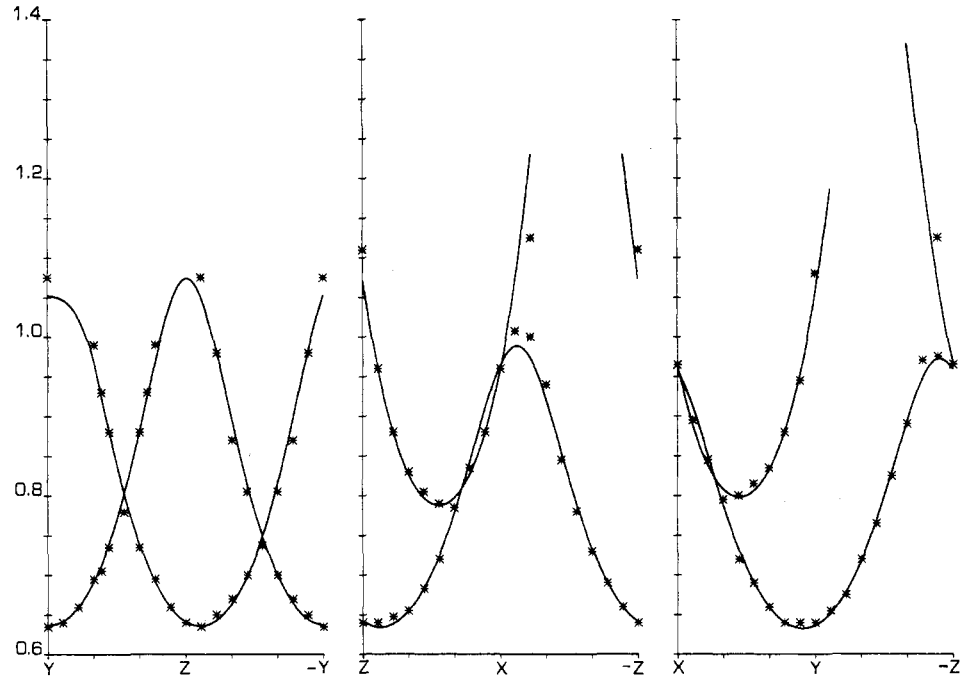

Figure 9. Angular dependence of the transition fields of $Mn(F_6acac)_2(proxyl)_2$ (II) at Q-band frequency at 140 K, in three orthogonal planes. *X*, *Y*, and *Z* are laboratory axes, with *X* parallel to a^* and *Z* orthogonal to the $01\bar{1}$ face.

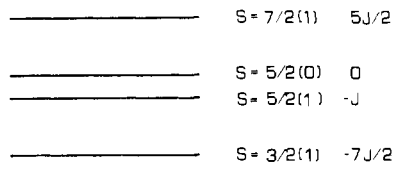

Figure 10. Order and energy separations of the spin levels for $Mn(F_6acac)_2(tempo)_2$ (I) and $Mn(F_6acac)_2(proxyl)_2$ (II).

If D_{r-r} is neglected, D_{Mn} and D_{Mn-r} can be calculated from the above expressions and the experimental *D* values for $S = {}^3/_2$ and for $S = {}^5/_2$. We find $D_{Mn-r} \simeq -0.36$ cm^{-1} and $D_{Mn} \simeq 0.25$ cm^{-1}. The sign of D_{Mn-r} is in agreement with a dipolar interaction, and the value compares well with that observed in $Cu(F_6acac)_2(tempol)$.[9] The value of D_{Mn} is slightly higher than that reported for the water adduct of $Mn(acac)_3$,[17] but, given the approximate nature of the above considerations, it can be considered as satisfactory.

Mechanism of Exchange. The coupling constants for I and II obtained by magnetic susceptibility and confirmed by EPR spectra are expected to be related to orbital interactions by the relation[16]

$$J_{Mn-r} = \frac{1}{S_r \cdot S_{Mn}}(J_{\pi,xy} + J_{\pi,x^2-y^2} + J_{\pi,xz} + J_{\pi,yz} + J_{\pi,z^2})$$

where $J_{\pi,i}$ indicates the exchange interaction between the unpaired electron on the radical and that in the i orbital of the metal. The site symmetry at the manganese(II) ion is only C_i, but the overall symmetry of the complex is not far from C_{2h}, the C_2 axis being in the equatorial plane and bisecting the large O–Mn–O angle.[10] I and II differ essentially in the Mn–O–N angle, which is 167° in the former and 145° for the latter. In C_{2h} symmetry only the *xy* and *xz* metal orbitals can yield bonding (antiferromagnetic) interactions with the ligand orbitals, while the others can only yield ferromagnetic interactions. The Mn–O–N angle is expected to affect the coupling because in the limit Mn–O–N = 180° the *xy* orbital becomes orthogonal to the π ligand orbitals, yielding a ferromagnetic coupling. This is in fact the situation found in several octahedral copper(II) adducts. Therefore, on this basis, we can expect a larger antiferromagnetic coupling for II than for I as experimentally found.[10]

Conclusions. The main result of this investigation is that fairly strong antiferromagnetic interactions can be established between transition-metal ions with more than one unpaired electron and organic radicals. The coupling, however, does not reach the strong-bonding limit, where only the lowest spin multiplicity state is thermally populated. The EPR spectra are temperature-dependent and consistent with the energy level pattern previously derived from magnetic susceptibility data. Analysis of the zero-field splittings of two different spin multiplets showed that both the local manganese(II) and the spin–spin dependent contributions determine the observed values. The result could be very important for the analysis of data of naturally occurring systems in which manganese(II) is coupled to semiquinone radicals.[22]

Registry No. I, 102046-42-4; II, 101998-08-7.

(22) Lynch, M. W.; Hendrickson, D. N.; Fitzgerald, B. J.; Pierpont, C. G. *J. Am. Chem. Soc.* **1984**, *106*, 2041.